molbank

MDPI

Short Note

Sumatriptan Succinate Hemi(Ethanol Solvate)

Petr A. Buikin [1,2], Anna V. Vologzhanina [1] and Alexander A. Korlyukov [1,*]

[1] A. N. Nesmeyanov Institute of Organoelement Compounds, Russian Academy of Sciences, 28 Vavilov St., Moscow 119334, Russia; vologzhanina@mail.ru (A.V.V.)
[2] N. S. Kurnakov Institute of General and Inorganic Chemistry, Russian Academy of Sciences, 31 Leninskii Prosp., Moscow 119991, Russia
* Correspondence: alex@xrlab.ineos.ac.ru

Abstract: 1-(3-(2-(Dimethylammonio)ethyl)-1H-indol-5-yl)-N-methylmethanesulfonamide succinate (sumatriptan succinate, $HSum^+ \cdot HSucc^-$) is a serotonin receptor agonist used to treat migraines. By the recrystallization of this substance from ethanol, its hemi(ethanol solvate), $HSum^+ \cdot HSucc^- \cdot 0.5EtOH$, was obtained. The solid was characterized by X-ray diffraction and FT-IR spectroscopy. In $HSum^+ \cdot HSucc^- \cdot 0.5EtOH$, solvent molecules link succinate anions into infinite O–H. . .O bonded chains, which are further connected by N–H. . .O interactions with cations into H-bonded layers.

Keywords: active pharmaceutical ingredient; H-bond propensity; single-crystal X-ray diffraction; sumatriptan

1. Introduction

Sumatriptan succinate ($HSum^+ \cdot HSucc^-$) is the active pharmaceutical ingredient of commercially available drugs Imitrex, Treximet and others used to treat migraine headaches and cluster headaches. In addition, its anti-inflammatory properties were also reported [1]. The corresponding free base Sumatriptan (Sum) like all triptans acts as a serotonin $5\text{-}HT_{1B}/5\text{-}HT_{1D}$ receptor agonist [2,3]. During its metabolism, Sum transforms into a glucuronide of indol-3-yl-acetic acid derivative via several steps [4]. The crystal structures of both Sum and $HSum^+ \cdot Hsucc^-$ were published before [5,6].

Taking into account the strong effect of solvent molecules on the properties of solids, such as solubility, tabletability, stability and others, the pharmaceutical industry is highly interested in the crystal structures of all solid forms of active pharmaceutical ingredients which can occur during drug production. This information is required for phase identification and purity control. In our study of novel solid forms of known active pharmaceutical ingredients [7–9], the ability of sumatriptan succinate to form various solvates was examined. Recrystallization from ethanol afforded a hemisolvate, $HSum^+ \cdot HSucc^- \cdot 0.5EtOH$ (**1**). Herein we report on the molecular and crystal structures of **1**, Scheme 1.

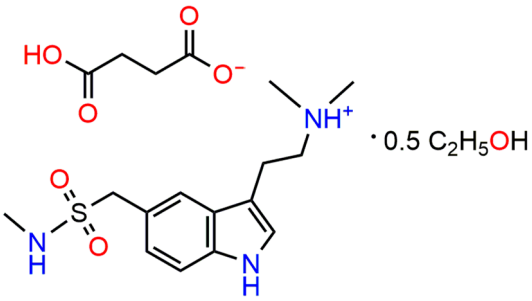

Scheme 1. Schematic representation of **1**.

check for updates

Citation: Buikin, P.A.; Vologzhanina, A.V.; Korlyukov, A.A. Sumatriptan Succinate Hemi(Ethanol Solvate). *Molbank* **2024**, *2024*, M1766. https://doi.org/10.3390/M1766

Academic Editor: René T. Boeré

Received: 22 November 2023
Revised: 20 December 2023
Accepted: 4 January 2024
Published: 26 January 2024

2. Results and Discussion

Sumatriptan succinate was dissolved in ethanol without purification. After several days of standing in air at r.t., orange prismatic crystals precipitated. The precipitate was filtered off and studied using single-crystal X-ray diffraction, FT-IR and NMR spectroscopy, as well as powder X-ray diffraction. The powder XRD pattern indicates that **1** is unstable upon milling. Milling under hexane protection results in full ethanol loss and the formation of a solvent free $HSum^{+}\cdot HSucc^{-}$ substance (Refcode ETITEG in the Cambridge Structural Database [10,11]). Rietveld refinement of the sample milled under ethanol protection revealed a mixture of **1** and $HSum^{+}\cdot HSucc^{-}$ in the 0.2:0.8 ratio. At the same time all crystals of the precipitate that was formed had the crystal parameters of the target form **1** and were further used to collect the FT-IR spectrum.

The asymmetric unit of **1** is represented in Figure 1. It contains two cations, two anions, and one ethanol molecule. The positions of H(C), H(N) and H(O) can be easily revealed from difference Fourier maps. Thus, protonation of the dimethylamine moiety of Sum and deprotonation of only one of two carboxylic groups of Succ was observed for all symmetrically independent species. Our conclusion about the positions of hydrogen atoms is supported by interatomic and intermolecular distances. Particularly, C–O distances for deprotonated carboxylic groups vary from 1.238(4) to 1.274(4) Å. These values are intermediate between C=O and C–O(H) bond lengths for protonated groups in **1** equal to, respectively, 1.207(4)–1.210(4) and 1.313(4)–1.315(4) Å.

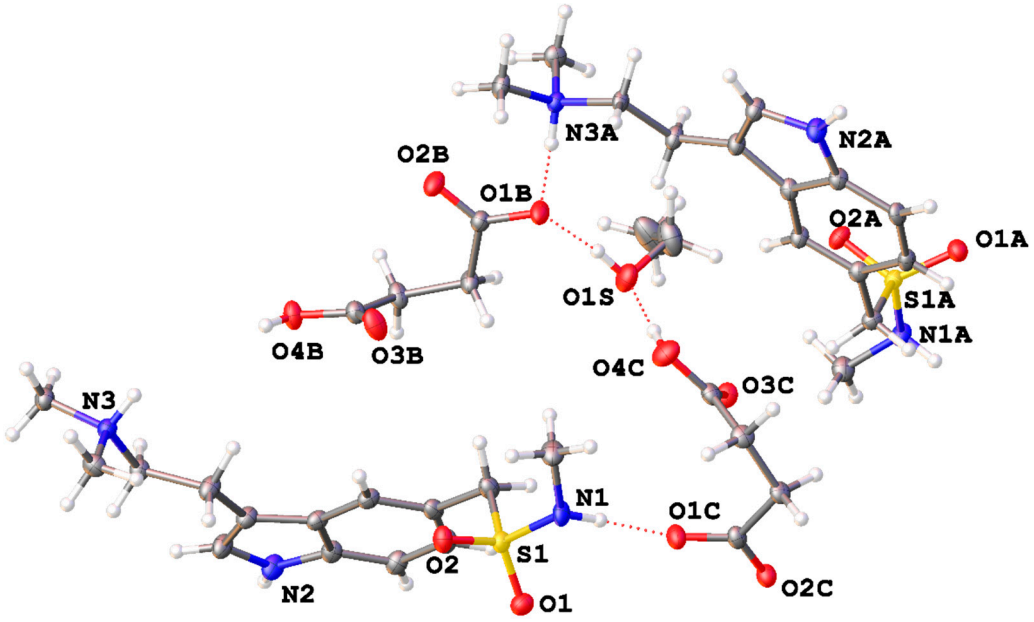

Figure 1. Asymmetric unit of **1** in representation of atoms with displacement ellipsoids (p = 50%).

The molecular conformations of cations in **1** are nearly identical with the average R.M.S.D for non-hydrogen atoms equal to 0.069 Å. In Figure 2, Sum conformations in different solid forms are compared by superimposing the non-hydrogen atoms of the bicycle. It is clearly seen that rotation along single C–C, S–N and C–N groups is possible so that disposition of dimethylammonioethyl (dimethylaminoethyl) and N-methylmethanesulfonamide groups in all solids is different. The staggered conformation of succinate anions in two solvatomorphs is nearly equal: the maximal deviation of non-hydrogen atoms is 0.639 Å only; the C–C–C–C torsion angle is c.a. 60°.

Different cation conformations should be associated with different H-bonded motifs. Both in Sum and in $HSum^{+}\cdot HSucc^{-}$ salts, the number of H-bond donors and acceptors is inequivalent, thus, different functional groups compete with each other to form the most stable H-bonding pattern. What is more, the presence of a solvent molecule in this case is expected only if the propensity of H-bond formation with this solvent is comparable

or higher than the propensity of H-bond formation between the functional groups of the main components [12]. The propensities of H-bond formation for the functional groups present in $HSum^+ \cdot HSucc^-$ salts with and without ethanol were estimated using the H-bond Propensities tool of the Mercury package [13] as described in Refs. [14,15]. The data obtained are listed in Table 1.

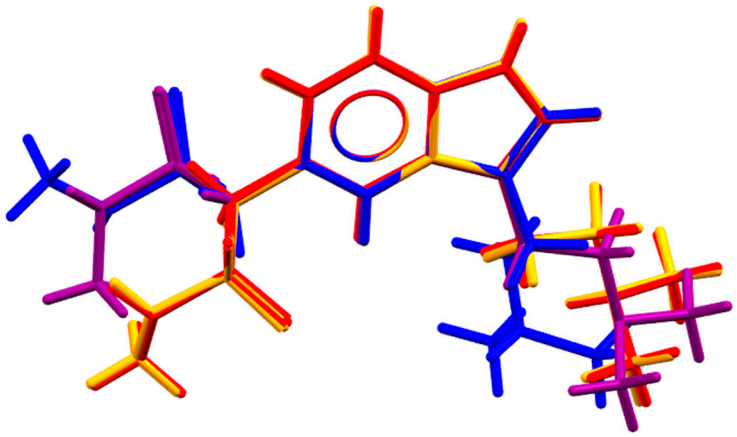

Figure 2. Molecular conformations of Sum and HSum+ in **1** (red and orange), $HSum^+ \cdot HSucc^-$ (ETITEG; blue) and free base Sum (DEFZEU; purple). Non-hydrogen atoms of the bicycle are superimposed.

Table 1. Propensities of H-bonding in $HSum^+ \cdot HSucc^-$ salts.

$HSum^+ \cdot HSucc^-$ (ETITEG [6])				**1**			
Donor	**Acceptor**	**Propensity**	**Observed**	**Donor**	**Acceptor**	**Propensity**	**Observed**
R-COOH	CO_2	0.85	Yes	R-COOH	CO_2	0.84	Yes
	SO_2	0.51			SO_2	0.46	
	COOH	0.33			COOH	0.26	
					R-OH	0.34	Yes
Ammonium R_3NH^+	CO_2	0.90	Yes	Ammonium R_3NH^+	CO_2	0.81	Yes
	SO_2	0.63			SO_2	0.43	
	COOH	0.43			COOH	0.23	
					R-OH	0.31	
Indole NH	CO_2	0.97	Yes	Indole NH	CO_2	0.87	
	SO_2	0.88			SO_2	0.52	
	COOH	0.79			COOH	0.31	Yes
					R-OH	0.40	
Sulfonamide SO_2NH	CO_2	0.92	Yes	Sulfonamide SO_2NH	CO_2	0.91	Yes
	SO_2	0.68			SO_2	0.62	
	COOH	0.50			COOH	0.40	
				ROH	CO_2	0.84	Yes
					SO_2	0.47	
					COOH	0.26	
					R-OH	0.34	

The evaluated propensities indicate that in $HSum^+ \cdot HSucc^-$ (ETITEG; [6]), all donors take part in H-bonding with the most likely acceptors. The presence of ethanol molecules becomes possible because it is as likely an H-bond donor as COOH and R_3NH groups. In **1**, two unlikely H-bonds are present, thus more stable polymorphs of this salt can exist. Fragments of experimentally obtained H-bonded networks in these two salts are compared in Figure 3. The parameters of H-bonds in solid $HSum^+ \cdot HSucc^- \cdot 0.5EtOH$ are listed in Table 2.

$HSucc^-$ anions form infinite chains in $HSum^+ \cdot HSucc^-$ (ETITEG; [6]) in accordance with the most likely H-bonds (red chains in Figure 3a). In $HSum^+ \cdot Hsucc^- \cdot 0.5EtOH$, ethanol molecules act as linkers within similar chains (red chains in Figure 3b). $HSum^+$ cations connect these chains into infinite frameworks and layers, respectively. In both solids, the cation acts as a three-connected node of an H-bonded network, and the anion is a five-

connected node. The resulting topologies of the underlying 3,5-c binodal H-bonded nets in these compounds evaluated with the ToposPro package [16] are, respectively, seh-3,5-P2_1/c and 3,5L24 (for notation of nets see Ref. [17]). Analysis of the H-bonding nets in the CSD using Topcryst service [18] indicates that these nets were previously met in, respectively, six and one hundred and seventy four organic solids.

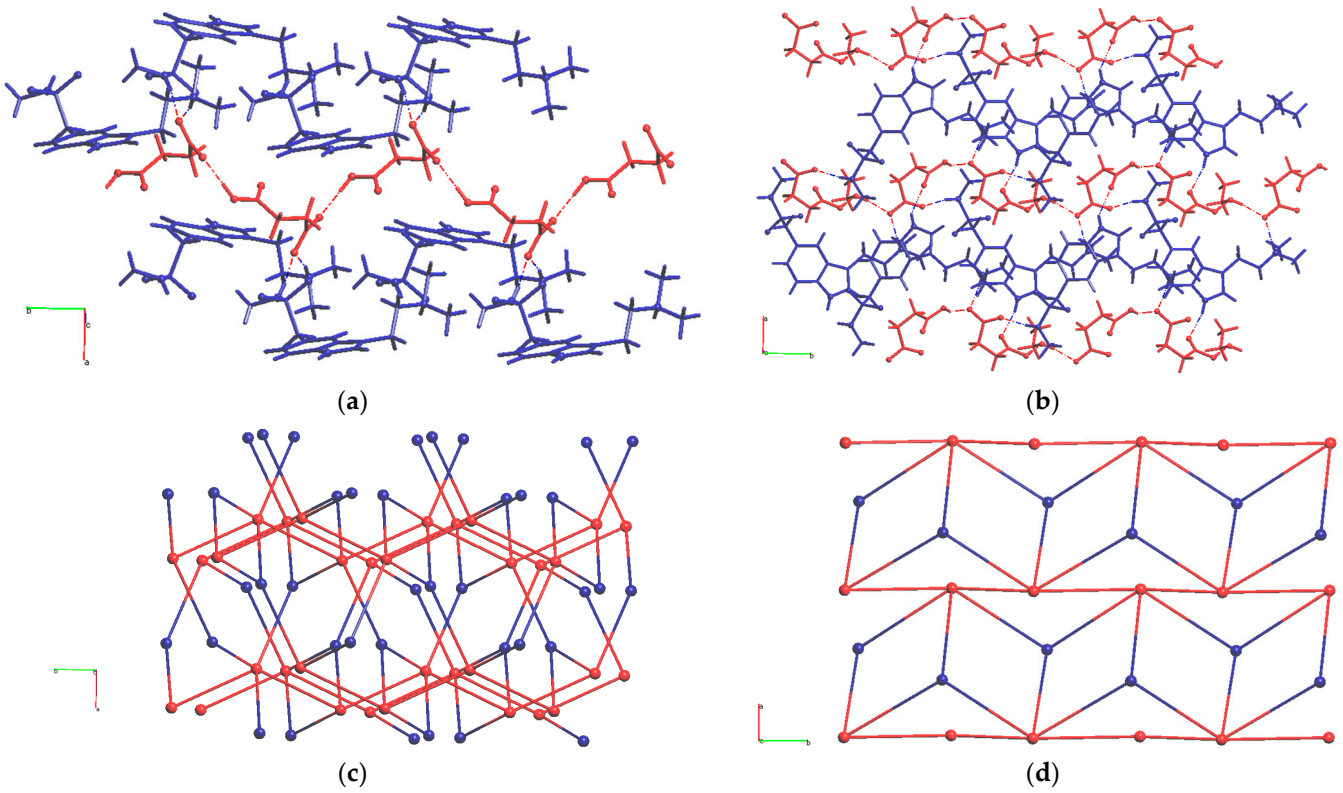

Figure 3. Fragment of H-bonded motifs in (**a**) $HSum^{+}{\cdot}HSucc^{-}$ (ETITEG; [6]), (**b**) 1. HSum+ and $HSucc^{-}$ ions are marked with blue and red, respectively. H-bonds are dashed. (**c**,**d**) Underlying H-bonded nets in the same salts.

Table 2. Hydrogen bonding parameters for **1** (Å, °).

	D–H···A	D–H	H···A	D···A	D–H···A
1	N(1)–H(1)···O(1C)	0.90(3)	1.95(3)	2.844(4)	173(4)
2	N(2)–H(2)···O(3B ^{i})	0.89(3)	2.07(3)	2.877(5)	151(3)
3	N(3)–H(3)···O(2C)	0.89(3)	1.81(3)	2.669(4)	162(3)
4	N(1A)–H(1AA)···O(2B ^{ii})	0.87(3)	1.95(3)	2.794(4)	163(4)
5	N(2A)–H(2AA)···O(3C ^{iii})	0.89(3)	2.06(3)	2.866(4)	161(1)
6	N(3A)–H(3A)···O(1B)	0.88(4)	1.80(4)	2.636(4)	158(5)
7	O(4C)–H(4C)···O(1S)	0.86(3)	1.68(3)	2.532(4)	170(4)
8	O(1S)–H(1S)···O(1B)	0.85(3)	1.78(3)	2.603(4)	162(5)
9	O(4B)–H(4B)···O(2C ^{iii})	0.84(4)	1.70(4)	2.526(4)	165(4)

Symmetry codes: (i) 1 + x, y, z; (ii) x, −1 + y, z; (iii) −1 + x, y, z.

To sum up, by recrystallization from ethanol, we obtained a novel solid form of sumatriptan succinate used to treat migraine and cluster headaches. Co-crystallization with ethanol is in accordance with the most likely H-bonds in a three-component mixture as estimated using the H-bond propensity tool, because the propensities of OH. . .O_2C and COOH. . .O_2C bonds were found to be similar. In both solids, the cations and anions act as three- and five-connected nodes, and ethanol molecules—as simple linkers between two anions. Nevertheless, the presence of solvent molecules strongly affects the overall

H-bonding network. In $HSum^{+}\cdot HSucc^{-}$, a 3D H-bonded framework is observed, while in $HSum^{+}\cdot HSucc^{-}\cdot 0.5EtOH$, 2D layers are found.

3. Materials and Methods

Fine powder of sumatriptan succinate obtained from Sigma Aldrich (Moscow, Russia; 0.012 g, 0.0046 mmol) was dissolved in 3 mL of water-ethanol mixture. Single crystals were grown by slow evaporation. NMR spectra (Figures S1–S7, SI) were obtained for ^{1}H at 400 MHz, for ^{13}C at 100 MHz and for ^{15}N at 40 MHz, using Bruker AVANCE III WB 400 spectrometer (Bruker, Billerica, MA, USA). FTIR spectrum (Figure S8, SI) was recorded on an IR spectrometer with a Fourier transformer Shimadzu IRTracer100 (Kyoto, Japan) in the range of 4000–600 cm^{-1} at a resolution of 1 cm^{-1} (Nujol mull, KBr pellets). The powder XRD data were recorded at Bruker D8 Advance diffractometer (Bruker, Billerica, MA, USA) equipped a LynxEye detector and Ge(111) monochromator in a transmission mode. CuKα radiation with a wavelength of 1.544493 Å was used. The 2θ range was 4.0–60.0° with a step size of 0.2° (Figure S9, SI).

X-ray Diffraction

The intensities of reflections were collected at the Centre for Molecular Studies of INEOS RAS with Bruker D8 QUEST diffractometer at 100 K (MoKα = 0.71072 Å, φ and ω-scans). The structure was solved by the dual-space algorithm [19] and refined by full-matrix least squares against F^2 as two component inversion twin (SHELXL program [20]) using OLEX2 package [21], scale factors for two components are equal to 0.32(7) and 0.68(7), respectively. Non-hydrogen atoms were refined in an anisotropic approximation. Hydrogen atoms at carbon ones were calculated and included in the refinement with $U_{iso}(H) = 1.2U_{eq}(C)$. Hydrogen atoms of N-H and O-H groups were located in difference Fourier maps and refined with unconstrained U_{iso} and fixed bond distances (0.88 and 0.85Å, respectively).

Crystal Data for $C_{19}H_{30}N_3O_{6.5}S$ (M = 436.52 g/mol): monoclinic, space group Pc (no. 7), a = 9.834(9), b = 12.609(10), c = 16.946(16) Å, α = 90, β = 90.94(3), γ = 90°, V = 2101(3) $Å^3$, Z = 4, μ = 0.198 mm^{-1}, D_{calc} = 1.380 g cm^{-3}, F(000) = 932, 22256 reflections measured ($4.0° \leq 2\Theta \leq 61.8°$), 10388 unique ($R_{int}$ = 0.0602, R_{sigma} = 0.0763) which were used in all calculations. The final R_1 was 0.0467 ($I > 2\sigma(I)$) and wR_2 was 0.1188 (all data).

Supplementary Materials: NMR and FTIR spectra, Rietveld plot, crystallographic data in Crystallographic Information File (CIF) format.

Author Contributions: Conceptualization, A.A.K.; methodology, P.A.B.; investigation, A.V.V. and P.A.B.; writing—A.A.K. and A.V.V.; funding acquisition, A.A.K. All authors have read and agreed to the published version of the manuscript.

Funding: This research was funded by the Russian Science Foundation, grant number 20-13-00241.

Data Availability Statement: The X-ray data are available at CCDC under ref. code CCDC 2306805.

Acknowledgments: Ministry of Science and Higher Education of the Russian Federation is acknowledged for providing access to scientific literature.

Conflicts of Interest: The authors declare no conflicts of interest.

References

1. Ala, M.; Ghasemi, M.; Mohammad Jafari, R.; Dehpour, A.R. Beyond Its Anti-Migraine Properties, Sumatriptan Is an Anti-Inflammatory Agent: A Systematic Review. *Drug Devel. Res.* **2021**, *82*, 896–906. [CrossRef] [PubMed]
2. Syed, Y.Y. Sumatriptan/Naproxen Sodium: A Review in Migraine. *Drugs* **2016**, *76*, 111–121. [CrossRef] [PubMed]
3. Tfelt-Hansen, P.; De Vries, P.; Saxena, P.R. Triptans in Migraine. *Drugs* **2000**, *60*, 1259–1287. [CrossRef] [PubMed]
4. Pöstges, T.; Lehr, M. Metabolism of Sumatriptan Revisited. *Pharmacol. Res. Perspect.* **2023**, *11*, e01051. [CrossRef]
5. Ravikumar, K.; Sridhar, B.; Krishnan, H. Sumatriptan, an Anti migraine Drug. *Acta Cryst. Sect. E* **2006**, *62*, o1086–o1088. [CrossRef]
6. Ravikumar, K.; Swamy, G.Y.S.K.; Krishnan, H. α-{3-[2-(Di methyl ammonio) ethyl]-1H-Indol-5-Yl}-N-Methyl methanesulfon amide Succinate (Sumatriptan Succinate). *Acta Cryst. Sect. E* **2004**, *60*, o618–o620. [CrossRef]

7. Korlyukov, A.A.; Dorovatovskii, P.V.; Vologzhanina, A.V. N-(4-Methyl-3-((4-(Pyridin-3-Yl)Pyrimidin-2-Yl)Amino)Phenyl)-4-((4-Methylpiperazin-1-Yl)Methyl)Benzamide. *Molbank* **2022**, *2022*, M1461. [CrossRef]
8. Korlyukov, A.A.; Buikin, P.A.; Dorovatovskii, P.V.; Vologzhanina, A.V. Synthesis, NoSpherA2 Refinement, and Noncovalent Bonding of Abiraterone Bromide Monohydrate. *Struct. Chem.* **2023**, *34*, 1927–1934. [CrossRef]
9. Buikin, P.; Vologzhanina, A.; Novikov, R.; Dorovatovskii, P.; Korlyukov, A. Abiraterone Acetate Complexes with Biometals: Synthesis, Characterization in Solid and Solution, and the Nature of Chemical Bonding. *Pharmaceutics* **2023**, *15*, 2180. [CrossRef]
10. Groom, C.R.; Bruno, I.J.; Lightfoot, M.P.; Ward, S.C. The Cambridge Structural Database. *Acta Cryst. Sect. B* **2016**, *72*, 171–179. [CrossRef]
11. Taylor, R.; Wood, P.A. A Million Crystal Structures: The Whole Is Greater than the Sum of Its Parts. *Chem. Rev.* **2019**, *119*, 9427–9477. [CrossRef] [PubMed]
12. Delori, A.; Galek, P.T.A.; Pidcock, E.; Jones, W. Quantifying Homo- and Heteromolecular Hydrogen Bonds as a Guide for Adduct Formation. *Chem. Eur. J.* **2012**, *18*, 6835–6846. [CrossRef] [PubMed]
13. Macrae, C.F.; Sovago, I.; Cottrell, S.J.; Galek, P.T.A.; McCabe, P.; Pidcock, E.; Platings, M.; Shields, G.P.; Stevens, J.S.; Towler, M.; et al. Mercury 4.0: From Visualization to Analysis, Design and Prediction. *J. Appl. Cryst.* **2020**, *53*, 226–235. [CrossRef] [PubMed]
14. Galek, P.T.A.; Allen, F.H.; Fábián, L.; Feeder, N. Knowledge-Based H-Bond Prediction to Aid Experimental Polymorph Screening. *CrystEngComm* **2009**, *11*, 2634–2639. [CrossRef]
15. Sarkar, N.; Sinha, A.S.; Aakeröy, C.B. Systematic Investigation of Hydrogen-Bond Propensities for Informing Co-Crystal Design and Assembly. *CrystEngComm* **2019**, *21*, 6048–6055. [CrossRef]
16. Shevchenko, A.P.; Blatov, V.A. Simplify to Understand: How to Elucidate Crystal Structures? *Struct. Chem.* **2021**, *32*, 507–519. [CrossRef]
17. Blatov, V.A.; O'Keeffe, M.; Proserpio, D.M. Vertex-, Face-, Point-, Schläfli-, and Delaney-Symbols in Nets, Polyhedra and Tilings: Recommended Terminology. *CrystEngComm* **2010**, *12*, 44–48. [CrossRef]
18. Shevchenko, A.P.; Shabalin, A.A.; Karpukhin, I.Y.; Blatov, V.A. Topological Representations of Crystal Structures: Generation, Analysis and Implementation in the *TopCryst* System. *Sci. Technol. Adv. Mat. Methods* **2022**, *2*, 250–265. [CrossRef]
19. Sheldrick, G.M. SHELXT—Integrated Space-Group and Crystal-Structure Determination. *Acta Cryst. Sect. A* **2015**, *A71*, 3–8. [CrossRef]
20. Sheldrick, G.M. Crystal Structure Refinement with SHELXL. *Acta Cryst. Sect. C* **2015**, *C71*, 3–8. [CrossRef]
21. Dolomanov, O.V.; Bourhis, L.J.; Gildea, R.J.; Howard, J.A.K.; Puschmann, H. OLEX2: A Complete Structure Solution, Refinement and Analysis Program. *J. Appl. Cryst.* **2009**, *42*, 339–341. [CrossRef]